INTERNATIONAL JOURNAL FOR NUMERICAL METHODS IN ENGINEERING, VOL. 30, 541–564 (1990)

FINITE ELEMENTS WITH DISPLACEMENT INTERPOLATED EMBEDDED LOCALIZATION LINES INSENSITIVE TO MESH SIZE AND DISTORTIONS

EDUARDO N. DVORKIN

Instituto de Materiales y Estructuras, Facultad de Ingeniería, Universidad de Buenos Aires, Buenos Aires, Argentina

and

Center for Industrial Research, Siderca, Buenos Aires, Argentina

ALBERTO M. CUITIÑO AND GUSTAVO GIOIA*

Instituto de Materiales y Estructuras, Facultad de Ingeniería, Universidad de Buenos Aires, Buenos Aires, Argentina

SUMMARY

A new finite element formulation aimed at the solution of problems involving strain localization is presented. The proposed formulation incorporates displacement interpolated embedded localization lines. Results are shown to converge to an 'exact solution' when the mesh is refined and also to be quite insensitive to mesh distortions.

1. INTRODUCTION

The phenomenon of strain localization is typical of a number of engineering problems involving a wide variety of materials. Some examples are blunt fracture in concrete, rocks and metals[1–3] and shear-band deformation in ductile metals.[4–6] Once localization is triggered, almost all the deformation concentrates within a band; this process will eventually lead to fracture. Although localization can be triggered by different physical mechanisms, depending on the type of material and tenso-deformational state,[5–8] from a phenomenological viewpoint it generally seems to be related to a non-positive definite tangent constitutive matrix, namely to *strain softening*. As limiting cases we can mention an abrupt stress drop for the fracture of highly brittle materials like glass, and an infinite stress plateau for the shear-band deformation of ductile materials like mild steel. Blunt fracture of concrete, rocks and ceramics presents a real strain softening in the load–displacement response by which a gradual vanishing of load operates during the fracture progress. A local constitutive relation showing strain softening was proved to be thermodynamically unacceptable.[9,10] From a macroscopic viewpoint, strain softening could be considered[11] as an expedient model to accomplish a homogeneous representation of a heterogeneous microstructure.

*CONICET Fellow

0029–5981/90/110541–24$12.00

Received 1 September 1989
Revised 12 January 1990

In this paper we are concerned with the finite element modelling of localization problems. It is important to note here that we use the term *localization* to refer to those cases in which the strain concentration in the form of bands is related to the behaviour of the material, rather than to the distribution of loads and boundary conditions.

Most of the available finite element techniques for dealing with strain localization problems were developed in the context of brittle failure of concrete. From these studies we know that the main difficulty caused by strain softening is the mesh size sensitivity, and that this problem can be avoided by the introduction of a fractomechanics concept: the *fracture energy*, i.e. the energy consumed in the opening of a unit area of localized fracture. This criterion requires the fracture energy to be considered as a material property which cannot depend on the chosen finite element mesh.[3,11,12] Regarding these considerations two main development routes, which are closely related,[13] have been proposed.

1. The smeared crack approach[14–16]

In this approach an average stress–strain relation that assures a correct fracture energy dissipation is specified for a band of *smeared cracks* of constant width, where this width is considered to be a material property related to the inhomogeneities size. Requiring the finite elements size to be equal to the band width results in the simplest modelling criterion. It was found by numerical experimentation that different finite element sizes can be used, provided the average stress–strain relation is adjusted so as to assure the correct fracture energy dissipation. So defined, the smeared crack approach gives objective results with regard to mesh size when using non-distorted finite elements. However, the behaviour is not clear when mesh distortions are necessary for modelling requirements; remarkably in these cases a correct energy dissipation cannot be assured, even when the mesh size tends to zero.[17]

2. The discrete crack approach[18,19]

In this approach, a stress–displacement relation is specified for the *discrete crack*, i.e. for the localization assumed with no width. The softening modulus is chosen so as to assure the correct energy dissipation. For localization problems this approach is quite equivalent to the smeared crack approach.[11] In the available finite element implementations of the discrete crack, the localization is assumed to take place between elements. When the localization extends through a certain node, this node must be split into two in order to allow the new crack element insertion. The need for repeated changes in the topological connectivity of the mesh is a very serious drawback of this implementation.

In both approaches the analyst must specify the following material properties:

(i) stress (strain) criterion for fracture initiation;
(ii) fracture energy.

Other formulations aimed at modelling strain localization problems are found in the literature. In References 4 and 20 a localization zone of constant width is embedded inside the finite element where localization has been triggered. The strains related to this band are simply averaged over all the element domain and afterwards superposed on the elastic strain field. This approach was not shown to be objective with regard to distortions in general quadrilateral elements. In Reference 5 a set of localized strain modes is included in the element formulation. Although this

formulation is without doubt very interesting for modelling shear-band deformation, it seems to be inadequate for fracture problems. In fact, the use of local softening stress–strain relations does not allow the fracture energy to be preserved. In Reference 7 also discontinuous strain fields are embedded in the elements. Finally, in Reference 17 a technique for using the smeared crack approach in distorted elements is presented.

Our present objective is to develop a finite element formulation for strain localization problems that:

1. Retains the desirable features of the smeared crack approach, namely the ability to model the progression of strain localization zones without remeshing and, for fracture problems, the use of an energy criterion in order to obtain results objective with regard to mesh refinement.
2. Achieves the additional capability of being objective with regard to mesh distortions, thus assuring the correct energy dissipation in fracture problems, even when distorted elements are used.

In this paper we develop a finite element formulation that fulfils the proposed requirements. The main aspects in our new formulation are:

1. We consider that strain localization involves a complete element as the minimum information quantum[4,5,17] instead of working at the integration points level as is usual in most of the available techniques.
2. When strain localization is encountered inside a finite element, we consider it in the form of a displacement discontinuity line embedded in the element domain. This displacement discontinuity is realistic in brittle fracture cases,[21] but should not be interpreted in a micromechanics sense in blunt fracture situations (concrete, ceramics, etc.) and in shear-band deformation.
3. Once localization has been triggered in a given element, there are two different constitutive relations defining its mechanical behaviour. First, a stress–displacement law for the discontinuity line. For fracture problems, this law must be adjusted to the fracture energy value. Secondly, a conventional stress–strain law for the rest of the domain (hyperelasticity or hypoelasticity); e.g. the concrete constitutive relation developed in our References 22–24.
4. The resulting finite elements are non-conforming. Hence, for a reliable analysis capability, the elements must not contain spurious zero-energy modes and must satisfy Irons patch test.[25–31] As shown in Section 3, these requirements are fulfilled by the proposed formulation. It is important to note that for problems involving strain localization the patch test should refer to constant stress rather than constant strain situations.[5]

Finally, an important note is in order. The finite element formulation presented herein is aimed at a global description of the structural effects due to strain localization. Hence, it is not possible to obtain a detailed description of the stress field near the localization zone. Whenever such a description is sought, more sophisticated models can be used, for example non-local formulations.[32,33]

2. THE NEW FORMULATION

In this section we develop the incremental formulation for a 2D isoparametric finite element where a strain localization takes place. Without any lack in generality we assume that the only

non-linearities in the problem are due to material behaviour. Geometrical non-linearities should be treated in the usual way.[29]

We assume the general body shown in Figure 1 in equilibrium at time (load level) t. At this time the localization phenomenon has been already triggered, and is described in the form of a localization line. We seek the equilibrium configuration at time (load level) $t + \Delta t$, i.e. the configuration depicted in Figure 1. This configuration must satisfy the principle of virtual work,[29,34]

$$\int_{V_1} \delta \mathbf{e}^{T\,t+\Delta t}\boldsymbol{\sigma}\,\mathrm{d}V_1 + \int_{V_2} \delta \mathbf{e}^{T\,t+\Delta t}\boldsymbol{\sigma}\,\mathrm{d}V_2 = \int_{S_1} \delta \mathbf{u}^{T\,t+\Delta t}\mathbf{p}_1\,\mathrm{d}S_1 + \int_{S_2} \delta \mathbf{u}^{T\,t+\Delta t}\mathbf{p}_2\,\mathrm{d}S_2 + \int_{A_1} \delta \mathbf{u}^{T\,t+\Delta t}\mathbf{r}_1\,\mathrm{d}A_1 + \int_{A_2} \delta \mathbf{u}^{T\,t+\Delta t}\mathbf{r}_2\,\mathrm{d}A_2 \tag{1}$$

In the above, and using the nomenclature of Reference 29,

- $\mathbf{e}$: vector containing the Cartesian components of the incremental infinitesimal strain tensors;
- ${}^{t+\Delta t}\boldsymbol{\sigma}$: vector containing the Cartesian components of the stress tensor at time $t + \Delta t$;
- $\mathbf{u}$: vector containing the Cartesian components of the incremental displacements.

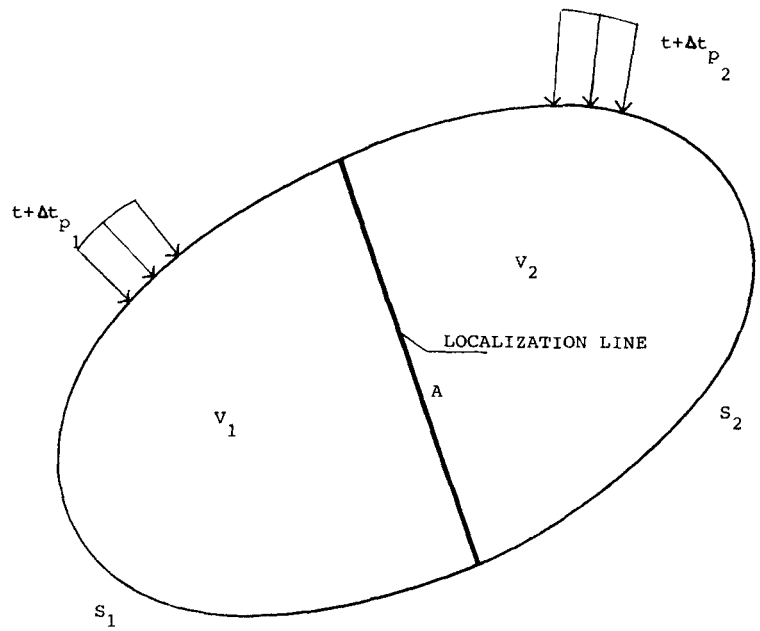

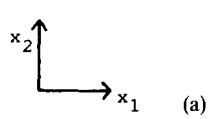

(a)

$V_1 + V_2 = V$

$S_1 + S_2 = S$

$A_1 = A_2 = A$

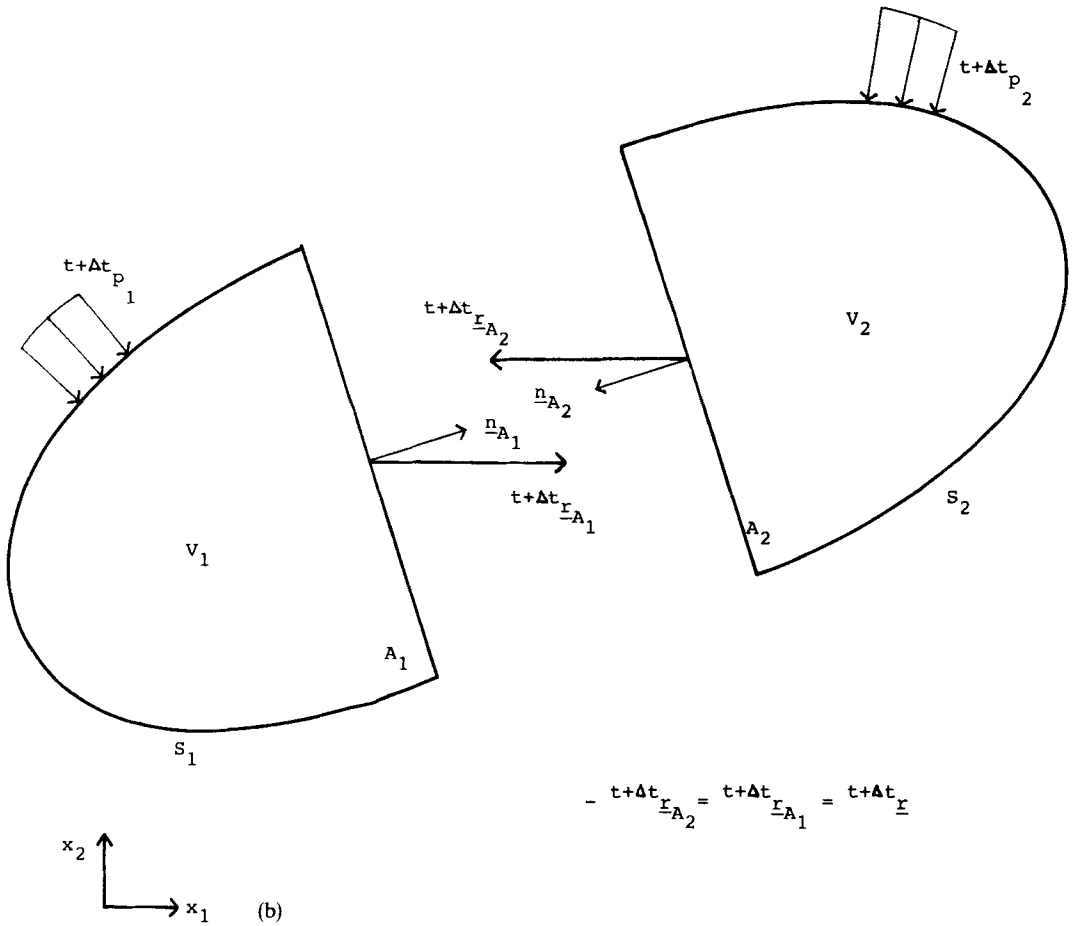

Figure 1. Solid with a localization line

For the others terms in equation (1), Figure 1 is self-explanatory.

We now introduce the displacement interpolation for the new finite element discretization. In order to obtain a first insight into the proposed formulation, we first analyse the simple case of a truss element with two nodes, which is shown in Figure 2(a). The incremental displacements interpolation prior to localization is given as usual, i.e.

$$u = \mathbf{H}\,\mathbf{U} \tag{2}$$

where $\mathbf{U}^{\mathrm{T}} = (U_1, U_2)$ is the vector of incremental nodal displacements and $\mathbf{H}$ is the displacement interpolation matrix.[29]

This interpolation is represented by line 3 in Figure 2(a). Once localization has been triggered, we consider a discontinuity of displacements at the element centre A, thus defining subdomains V_1 and V_2 as indicated in Figure 2(a). We assume V_2 to undergo a rigid relative incremental displacement U_c with respect to V_1. In order to obtain the same incremental displacement derivatives on both subdomains, we adopt for V_1 and V_2 the interpolations represented in Figure

2(a) by lines 1 and 2 respectively. Their mathematical expressions are

$$u_1 = \mathbf{H}\left[\mathbf{U} - \begin{pmatrix}0\\1\end{pmatrix} U^c\right] \tag{3}$$

for the left subdomain V_1 and

$$u_2 = \mathbf{H}\left[\mathbf{U} - \begin{pmatrix}0\\1\end{pmatrix} U^c\right] + U^c \tag{4}$$

for the right subdomain V_2. The purpose of matrix $\boldsymbol{\phi} = (0 \quad 1)^T$ in equations (3) and (4) is clear from the analysis of Figure 2(a). As expected, for every point either on V_1 or V_2 the incremental strain is

$$e = \mathbf{B}\left[\mathbf{U} - \begin{pmatrix}0\\1\end{pmatrix} U^c\right] = \mathbf{B}(\mathbf{U} - \boldsymbol{\phi} U^c) \tag{5}$$

where $\mathbf{B}$ is the usual strain–displacement matrix.[29]

For the 2D case in Figure 2(b), these concepts can be properly generalized by introducing the vector $\hat{\mathbf{U}}^c$ containing the components, in a local Cartesian system $(\hat{x}_1, \hat{x}_2)$, of the rigid incremental displacement associated with the localization line A,

$$\hat{\mathbf{U}}^c = \begin{bmatrix} \hat{v}^c \\ \hat{w}^c \end{bmatrix} \tag{6}$$

where $(\hat{x}_1, \hat{x}_2)$ is defined on the localization line, and thus depends on the localization criterion. If we call $\mathbf{R}$ the matrix that rotates Cartesian vector components from $(\hat{x}_1, \hat{x}_2)$ to the global Cartesian co-ordinates, the resulting displacement interpolation for the left subdomain V_1 can be written

$$\mathbf{u}_1 = \mathbf{H}(\mathbf{U} - \boldsymbol{\phi}\mathbf{R}\hat{\mathbf{U}}^c) \tag{7}$$

and for the right subdomain V_2

$$\mathbf{u}_2 = \mathbf{H}(\mathbf{U} - \boldsymbol{\phi}\mathbf{R}\hat{\mathbf{U}}^c) + \mathbf{R}\hat{\mathbf{U}}^c = \mathbf{H}\mathbf{U} - (\mathbf{H}\boldsymbol{\phi} - \mathbf{I})\mathbf{R}\hat{\mathbf{U}}^c \tag{8}$$

Matrix $\boldsymbol{\phi}$ in equation (7) and (8) follows from a straightforward generalization of its counterpart in equations (3) and (4). For 2D problems $\boldsymbol{\phi}$ can be written in the general form

$$\boldsymbol{\phi} = \begin{bmatrix} \boldsymbol{\phi}_1 \\ \vdots \\ \boldsymbol{\phi}_N \end{bmatrix} \tag{9}$$

where N is the number of nodes in the finite element, and each of the submatrices $\boldsymbol{\phi}_i$ of dimension (2×2) depends on the position of node i relative to the localization line, according to the following rule:

$$\boldsymbol{\phi}_i = \begin{cases} \mathbf{0} & \text{when node } i \in V_1 \\ \mathbf{I} & \text{when node } i \in V_2 \end{cases}$$

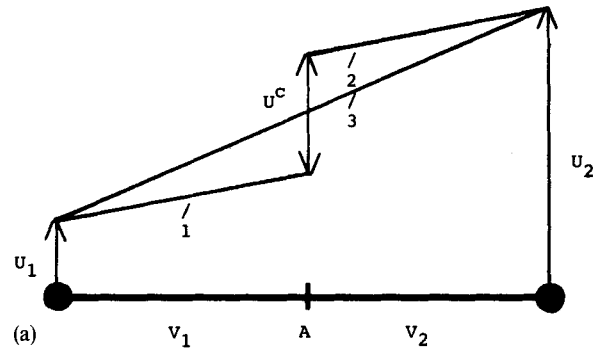

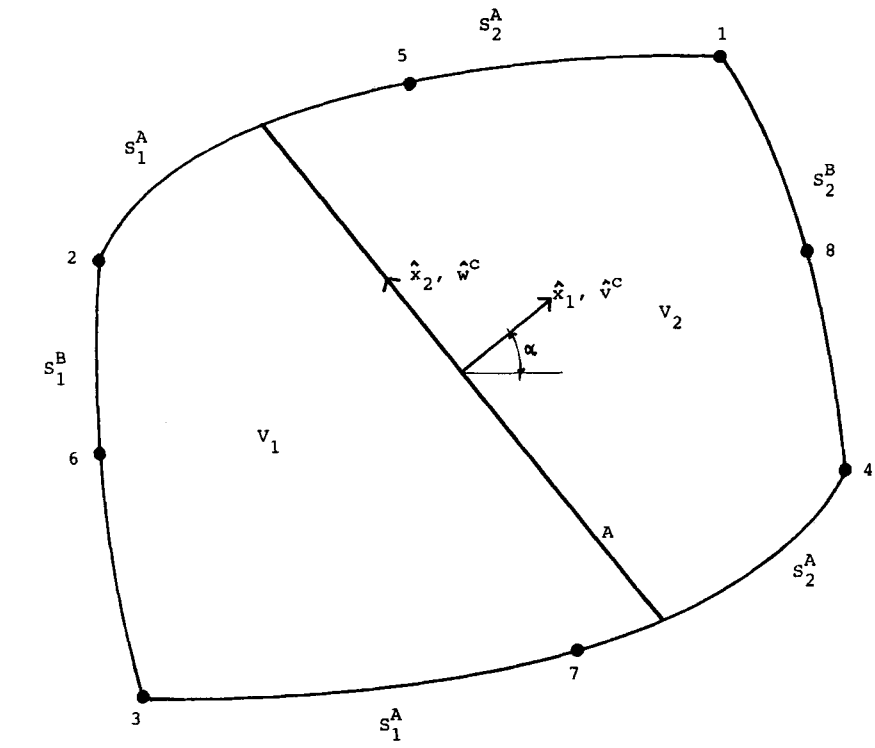

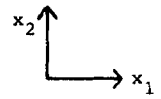

(b)

$$S_1 = S_1^A + S_1^B$$

$$S_2 = S_2^A + S_2^B$$

$$S_A = S_1^A + S_2^A$$

$$S_B = S_1^B + S_2^B$$

$$S = S_1 + S_2 \qquad V = V_1 + V_2$$

Figure 2. Finite element with embedded localization line: (a) 1D element; (b) 2D element

For two neighbouring points, one on the right and the other one on the left of the localization line, the incremental displacement discontinuity is given by

$$\mathbf{u}^+ - \mathbf{u}^- = \mathbf{R}\,\hat{\mathbf{U}}^c \tag{10}$$

Taking derivatives in equations (7) and (8) we obtain the same expression for the incremental strain. Therefore, for any point either on V_1 or V_2,

$$\mathbf{e} = \mathbf{B}(\mathbf{U} - \boldsymbol{\phi}\mathbf{R}\,\hat{\mathbf{U}}^c) \tag{11}$$

The displacement interpolation matrix for points on an element edge S_i is denoted $\mathbf{H}_{S_i}$. On the edge S_1^A,

$$\mathbf{u}_{S_1^A} = \mathbf{H}_{S_1^A}(\mathbf{U} - \boldsymbol{\phi}\mathbf{R}\,\hat{\mathbf{U}}^c) \tag{12a}$$

On the edge S_1^B, $\mathbf{H}_{S_1^B}\,\boldsymbol{\phi} = \mathbf{0}$, therefore on this edge,

$$\mathbf{u}_{S_1^B} = \mathbf{H}_{S_1^B}\mathbf{U} \tag{12b}$$

On the edge S_2^A,

$$\mathbf{u}_{S_2^A} = \mathbf{H}_{S_2^A}\mathbf{U} - (\mathbf{H}_{S_2^A}\boldsymbol{\phi} - \mathbf{I})\mathbf{R}\,\hat{\mathbf{U}}^c \tag{12c}$$

On the edge S_2^B, $\mathbf{H}_{S_2^B}\boldsymbol{\phi} = \mathbf{I}$, therefore on this edge,

$$\mathbf{u}_{S_2^B} = \mathbf{H}_{S_2^B}\mathbf{U} \tag{12d}$$

On the localization line, coming from the left,

$$\mathbf{u}_{A^-} = \mathbf{H}_A(\mathbf{U} - \boldsymbol{\phi}\mathbf{R}\,\hat{\mathbf{U}}^c) \tag{12e}$$

and coming from the right,

$$\mathbf{u}_{A^+} = \mathbf{H}_A\mathbf{U} - (\mathbf{H}_A\boldsymbol{\phi} - \mathbf{I})\mathbf{R}\,\hat{\mathbf{U}}^c \tag{12f}$$

Therefore, the different variations in equation (1) can be calculated in the finite element scheme as

$$\delta\mathbf{e} = \mathbf{B}(\delta\mathbf{U} - \boldsymbol{\phi}\mathbf{R}\,\delta\hat{\mathbf{U}}^c) \tag{13a}$$

$$\delta\mathbf{u}_{S_1^A} = \mathbf{H}_{S_1^A}(\delta\mathbf{U} - \boldsymbol{\phi}\mathbf{R}\,\delta\hat{\mathbf{U}}^c) \tag{13b}$$

$$\delta\mathbf{u}_{S_1^B} = \mathbf{H}_{S_1^B}\delta\mathbf{U} \tag{13c}$$

$$\delta\mathbf{u}_{S_2^A} = \mathbf{H}_{S_2^A}\delta\mathbf{U} - (\mathbf{H}_{S_2^A}\boldsymbol{\phi} - \mathbf{I})\mathbf{R}\,\delta\hat{\mathbf{U}}^c \tag{13d}$$

$$\delta\mathbf{u}_{S_2^B} = \mathbf{H}_{S_2^B}\delta\mathbf{U} \tag{13e}$$

$$\delta\mathbf{u}_{A^-} = \mathbf{H}_A(\delta\mathbf{U} - \boldsymbol{\phi}\mathbf{R}\,\delta\hat{\mathbf{U}}^c) \tag{13f}$$

$$\delta\mathbf{u}_{A^+} = \mathbf{H}_A\delta\mathbf{U} - (\mathbf{H}_A\boldsymbol{\phi} - \mathbf{I})\mathbf{R}\,\delta\hat{\mathbf{U}}^c \tag{13g}$$

Replacing in equation (1) and taking into account that $\delta\mathbf{U}$ and $\delta\hat{\mathbf{U}}^c$ are independent variations, after some algebra we arrive at the following two sets of equations:

$$\int_V \mathbf{B}^{\mathrm{T}\,t+\Delta t}\boldsymbol{\sigma}\,\mathrm{d}V = \int_S \mathbf{H}^{\mathrm{T}\,t+\Delta t}\mathbf{p}\,\mathrm{d}S \tag{14a}$$

$$\mathbf{R}^{\mathrm{T}}\boldsymbol{\phi}^{\mathrm{T}}\int_V \mathbf{B}^{\mathrm{T}\,t+\Delta t}\boldsymbol{\sigma}\,\mathrm{d}V = \mathbf{R}^{\mathrm{T}}\boldsymbol{\phi}^{\mathrm{T}}\int_{S^A} \mathbf{H}_{S^A}^{\mathrm{T}\,t+\Delta t}\mathbf{p}\,\mathrm{d}S^A - \int_{S_2^A}\mathbf{R}^{\mathrm{T}}\mathbf{p}_2\,\mathrm{d}S_2^A + \int_A {}^{t+\Delta t}\hat{\mathbf{f}}\,\mathrm{d}A \tag{14b}$$

The first set above is the usual set of global equilibrium equations, while the second set represents an additional requirement that we are now going to investigate. Taking into account that

$$\int_{S^A} \mathbf{H}_{S^A}^{T\,t+\Delta t}\mathbf{p}\,dS^A + \int_{S^B} \mathbf{H}_{S^B}^{T\,t+\Delta t}\mathbf{p}\,dS^B = \int_S \mathbf{H}_S^{T\,t+\Delta t}\mathbf{p}\,dS \tag{15}$$

and replacing with equations (14a) and (15) in equation (14b) we obtain

$$\mathbf{R}^T\boldsymbol{\phi}^T \int_{S^B} \mathbf{H}_{S^B}^{T\,t+\Delta t}\mathbf{p}\,dS^B + \int_{S_2^A} \mathbf{R}^T\mathbf{p}_2\,dS_2^A = \int_A {}^{t+\Delta t}\hat{\mathbf{r}}\,dA \tag{16}$$

Since

$$\mathbf{R}^T\boldsymbol{\phi}^T \int_{S^B} \mathbf{H}_{S^B}^{T\,t+\Delta t}\mathbf{p}\,dS^B = \mathbf{R}^T\boldsymbol{\phi}^T \int_{S_2^B} \mathbf{H}_{S_2^B}^{T\,t+\Delta t}\mathbf{p}_2\,dS_2^B \tag{17}$$

and since $\boldsymbol{\phi}^T\mathbf{H}_{S_2^B}^T = \mathbf{I}$, we finally obtain

$$\int_{S_2} \mathbf{R}^{T\,t+\Delta t}\mathbf{p}_2\,dS_2 = \int_A {}^{t+\Delta t}\hat{\mathbf{r}}\,dA \tag{18}$$

We now impose as an additional condition: the global equilibrium of each of the two parts into which the localization line subdivides the element, i.e.

$$\int_{S_2} \mathbf{R}^{T\,t+\Delta t}\mathbf{p}_2\,dS_2 = \int_A {}^{t+\Delta t}\underline{\boldsymbol{\sigma}}\cdot\mathbf{n}_A\,dA \tag{19}$$

where ${}^{t+\Delta t}\underline{\boldsymbol{\sigma}}$ is a second order tensor, $\mathbf{n}_A$ is a unit vector normal to the localization line and the dot indicates a scalar product. By properly defining a matrix $\boldsymbol{\psi}$ we can write

$${}^{t+\Delta t}\underline{\boldsymbol{\sigma}}\cdot\mathbf{n}_A = \boldsymbol{\psi}\,{}^{t+\Delta t}\boldsymbol{\sigma} \tag{20}$$

By substitution of equation (19) in equation (18) and taking into account equation (20), we obtain

$$\int_A \boldsymbol{\psi}\,{}^{t+\Delta t}\boldsymbol{\sigma}\,dA = \int_A {}^{t+\Delta t}\hat{\mathbf{r}}\,dA \tag{21}$$

Hence, and considering that at t the equilibrium equations are fulfilled, the second set of equations can be written in incremental form as

$$\int_A \boldsymbol{\psi}\,{}_t\boldsymbol{\sigma}\,dA = \int_A {}_t\hat{\mathbf{r}}\,dA \tag{22}$$

where ${}_t\boldsymbol{\sigma}$ and ${}_t\hat{\mathbf{r}}$ are increments. In order to satisfy equation (22) an iterative scheme is used at the element level.

For the linearized incremental step

$${}^{t+\Delta t}\boldsymbol{\sigma} = {}^t\boldsymbol{\sigma} + {}_t\mathbf{C}\mathbf{e} \tag{23}$$

where ${}_t\mathbf{C}$ is the tangent constitutive relation.

Using equations (11) and (23) in equation (14a) we obtain the global set of equilibrium equations:

$$\int_V \mathbf{B}^T{}_t\mathbf{C}\,\mathbf{B}(\mathbf{U} - \boldsymbol{\phi}\mathbf{R}\,\hat{\mathbf{U}}^c)\,dV = {}^{t+\Delta t}\mathbf{P} - {}^t\mathbf{F} \tag{24a}$$

where

$$^{t+\Delta t}\mathbf{P} = \int_S \mathbf{H}^{\mathrm{T}}\, {}^{t+\Delta t}\mathbf{p}\, \mathrm{d}S \tag{24b}$$

$$^{t}\mathbf{F} = \int_V \mathbf{B}^{\mathrm{T}}\, {}^{t}\boldsymbol{\sigma}\, \mathrm{d}V \tag{24c}$$

The right hand side of equation (24a) is the incremental load to evolve from the configuration at time t to the configuration at time $t + \Delta t$.

The stress–displacement incremental relation for the localization line is

$$_{t}\hat{\mathbf{f}} = {}_{t}\hat{\mathbf{C}}^{\mathrm{c}}\, \hat{\mathbf{U}}^{\mathrm{c}} \tag{25}$$

As we stated above, in fracture problems the definition of equation (25) is made so as to assure a correct energy dissipation.

Hence, replacing in equation (22) with equations (23) and (25) we obtain

$$\left[\int_A \boldsymbol{\psi}\, {}_{t}\mathbf{C}\, \mathbf{B}\, \mathrm{d}A\right]\mathbf{U} = \left[\int_A (\boldsymbol{\psi}\, {}_{t}\mathbf{C}\, \mathbf{B}\boldsymbol{\phi}\mathbf{R} + {}_{t}\hat{\mathbf{C}}^{\mathrm{c}})\, \mathrm{d}A\right]\hat{\mathbf{U}}^{\mathrm{c}} \tag{26}$$

Calling

$$\mathbf{S}_{uu} = \int_A \boldsymbol{\psi}\, {}_{t}\mathbf{C}\, \mathbf{B}\, \mathrm{d}A \tag{27a}$$

and

$$\mathbf{S}_{cc} = \int_A (\boldsymbol{\psi}\, {}_{t}\mathbf{C}\, \mathbf{B}\boldsymbol{\phi}\mathbf{R} + {}_{t}\hat{\mathbf{C}}^{\mathrm{c}})\, \mathrm{d}A \tag{27b}$$

we obtain

$$\hat{\mathbf{U}}^{\mathrm{c}} = \mathbf{S}_{cc}^{-1}\, \mathbf{S}_{uu}\, \mathbf{U} \tag{27c}$$

Therefore, we can condense the degrees of freedom corresponding to the localization line at the element level. Using (27c) in equation (24a), we finally get for the linearized step

$$\left[\int_V \mathbf{B}^{\mathrm{T}}\, {}_{t}\mathbf{C}\, \mathbf{B}(I - \boldsymbol{\phi}\mathbf{R}\, \mathbf{S}_{cc}^{-1}\, \mathbf{S}_{uu})\, \mathrm{d}V\right]\mathbf{U} = {}^{t+\Delta t}\mathbf{P} - {}^{t}\mathbf{F} \tag{28}$$

The term between brackets in the left hand side of the above equation is the consistent tangent stiffness matrix for the new formulation.

The final equilibrium configuration corresponding to time $t + \Delta t$ is reached using iterative methods.[29,35] It is very important to note that the stiffness matrix obtained in equation (28) is non-symmetric. Since most finite element codes use only symmetric matrices, a non-symmetric stiffness matrix complicates the implementation of the present formulation in existing codes. Other problems giving rise to non-symmetric stiffness matrices have motivated the development of special techniques to replace the original non-symmetric stiffness matrices for symmetric ones without losing too much efficiency in the iterative schemes.[24,36] In our case, numerical experimentation indicates that when using only the symmetric part of the stiffness matrix, the efficiency of the iterative procedure is still acceptable (see next section).

In this section we presented the localization lines embedded in displacement-based finite elements; however, the localization lines can be embedded in finite elements based on different formulations. In the following section we present some results obtained using localization lines embedded in elements based on mixed interpolation of tensorial components.[25–28,37]

3. NUMERICAL EXPERIMENTATION

In this section, we present the numerical experimentation we performed using the new formulation. The numerical tests are geared to:

1. Illustrate on the objectivity of the formulation with regard to mesh distortions which is, as we stated in the Introduction, one of the main thrusts for the present formulation. In order to investigate this topic, we analyse:
   (i) constant stress problems. In the present context, these problems are equivalent to the patch test;
   (ii) a problem with a more complicated stress distribution.
2. Investigate the efficiency of the formulation when only the symmetric part of the stiffness matrix is used. In order to explore this topic, we solve simple cases using different iterative schemes,[29] resorting first to the consistent stiffness matrix and afterwards to its symmetric component only.

In the numerical examples presented in this section we considered the following material behaviour.

(i) For the localization line, a stress–displacement constitutive relation corresponding to Mode I blunt fracture:

$$\begin{bmatrix} {}_t\hat{r}_1 \\ {}_t\hat{r}_2 \end{bmatrix} = \begin{bmatrix} {}_tE_T({}^t\hat{v}_c) & 0 \\ 0 & {}_tG_T \end{bmatrix} \begin{bmatrix} \hat{v}_c \\ \hat{w}_c \end{bmatrix} \tag{29}$$

where, as indicated, modulus ${}_tE_T$ is a function of ${}^t\hat{v}_c$ and modulus ${}_tG_T$ is assumed to be constant. Figure 3 shows the two different functions ${}_tE_T({}^t\hat{v}_c)$ considered herein:[15,32] we have adjusted both functions to a fracture energy $G_F = 0{\cdot}2e - 4$. The fracture initiation criterion is shown in Figure 4, and is presented in Reference 24.

(ii) Outside the localization line, a linear elastic stress–strain relation. It is important to remark that any other constitutive relation can be used.

Constant stress problems

In Figures 5 to 8 we show the results corresponding to some constant stress problems. In these types of problem the localization has to be induced, therefore we slightly weakened the elements that are shadowed in the figures. In all cases the results show that the present formulation is objective with regard to mesh distortions. For the cases in Figures 6 and 8 (pure shear) it is worth noting that, since we only consider a Mode I localization type, the discontinuity lines are at an angle of 45° with the plate sides. The final equilibrium configurations were drawn amplifying the displacements 20 times.

Bending of a simply supported beam

In this case, where the stresses are not constant in the element domains, in order to perform a fair evaluation of the objectivity of the new formulation with regard to mesh distortions, it is fundamental to use finite elements that, in the absence of localization, provide objective results.

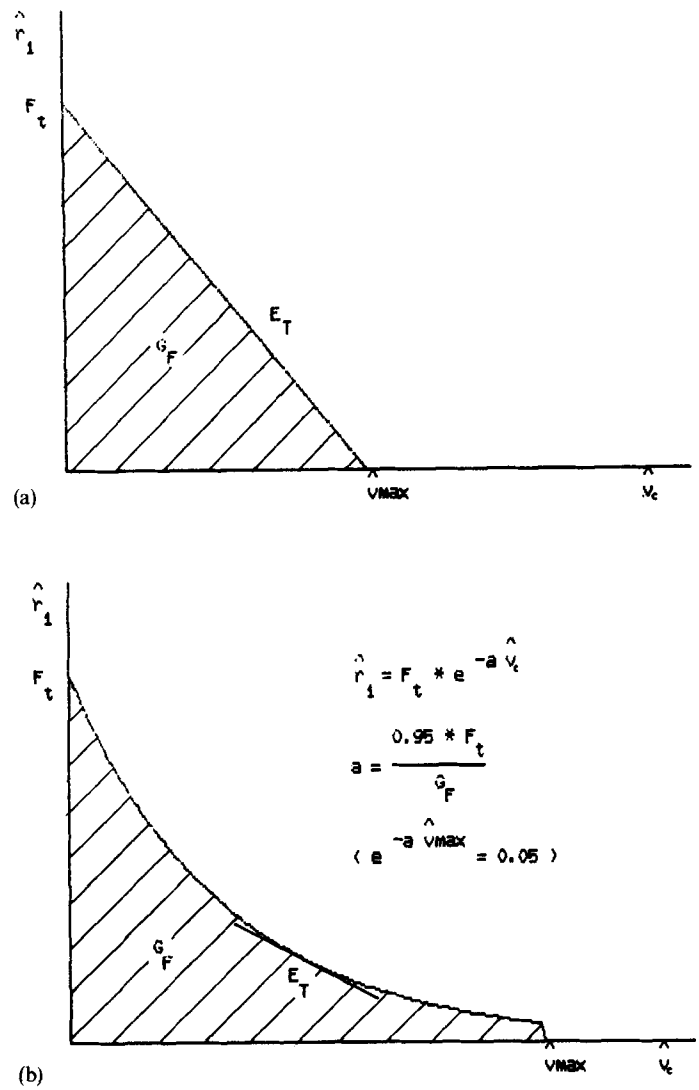

Figure 3. Some simple constitutive relations for the localization line: (a) linear model; (b) non-linear model

Considering that the standard isoparametric 4N and 8N elements do not fulfil objectivity with regard to mesh distortions, we use the quadrilateral QMITC element, based on mixed interpolation of tensorial components.[28,37]

In Figure 9 we show the results obtained using:

(i) standard 4N elements + new localization formulation;
QMITC elements + new localization formulation.

It is clear from these results that, in order to achieve objectivity with regard to mesh distortions, it is necessary to use the new formulation coupled to an element that is also quite insensitive to element distortions. The final equilibrium configurations were drawn amplifying the displacements 40 times.

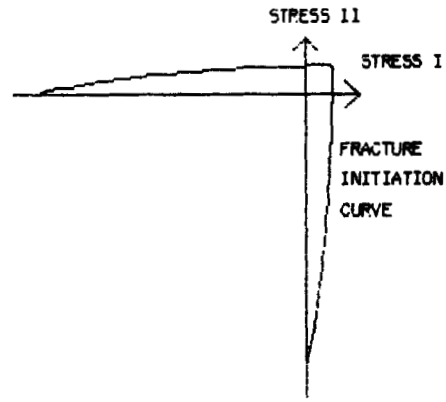

Figure 4. Blunt fracture initiation criterion

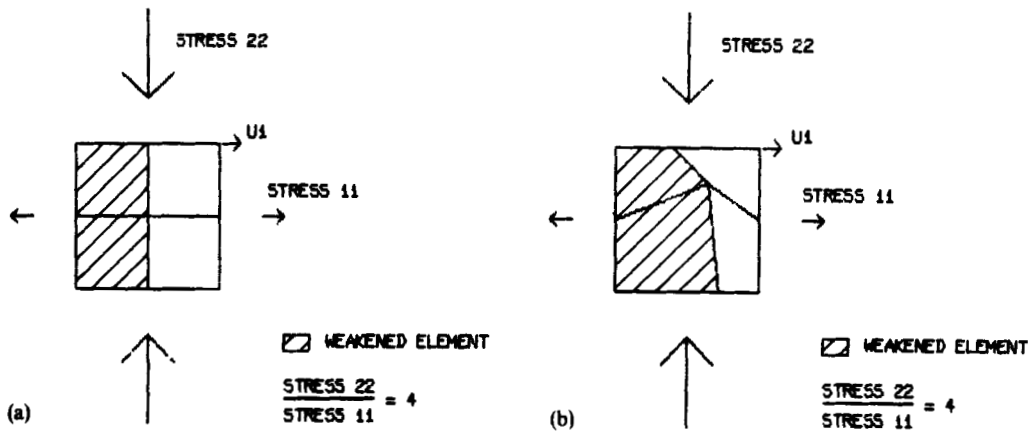

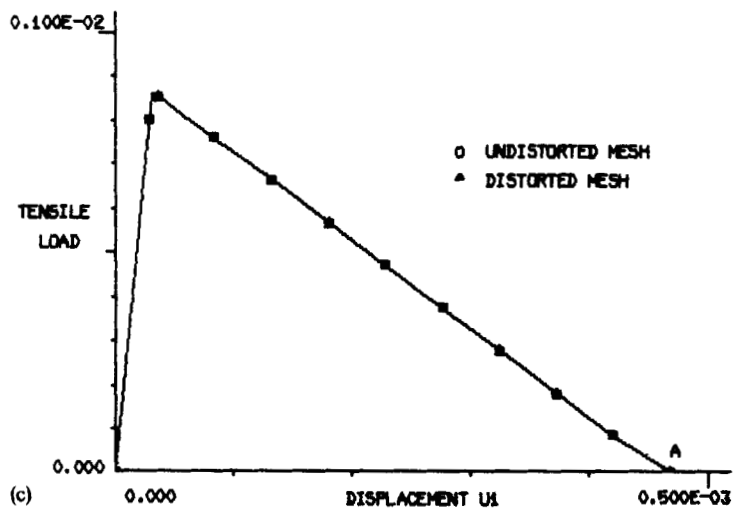

Figure 5(a, b, c)

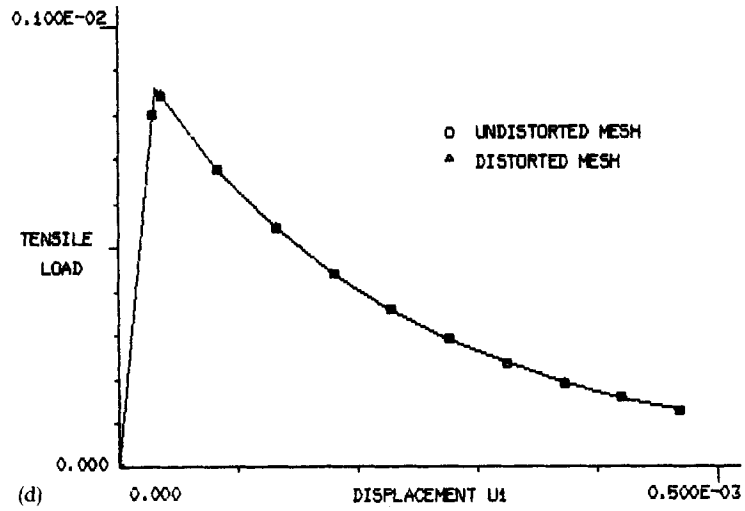

(d)

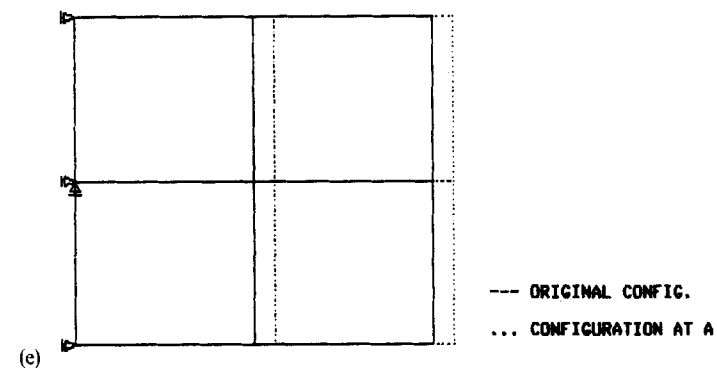

(e)

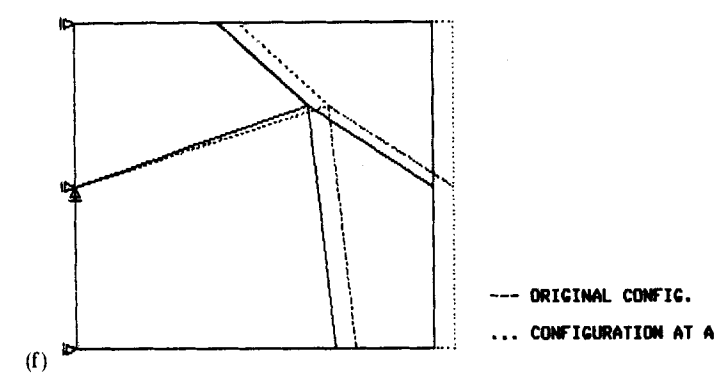

(f)

Figure 5. Biaxial stress state in four element meshes (plane stress): (a) undistorted mesh; (b) distorted mesh; (c) results corresponding to a linear $\hat{r}$–$\hat{v}$ relation; (d) results corresponding to a non-linear $\hat{r}$–$\hat{v}$ relation; (e) final equilibrium configuration of undistorted mesh; (f) final equilibrium configuration of distorted mesh

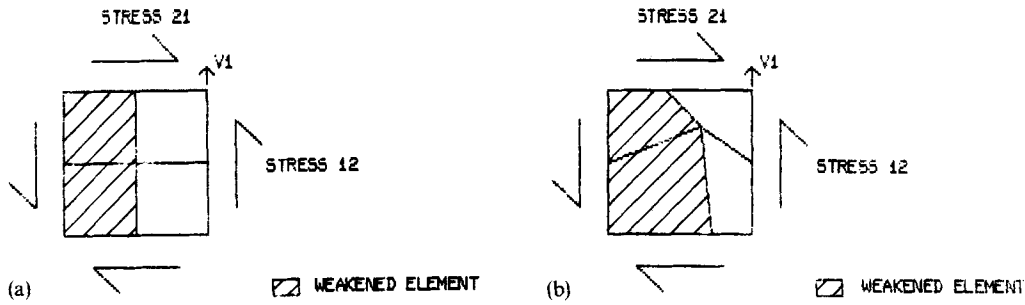

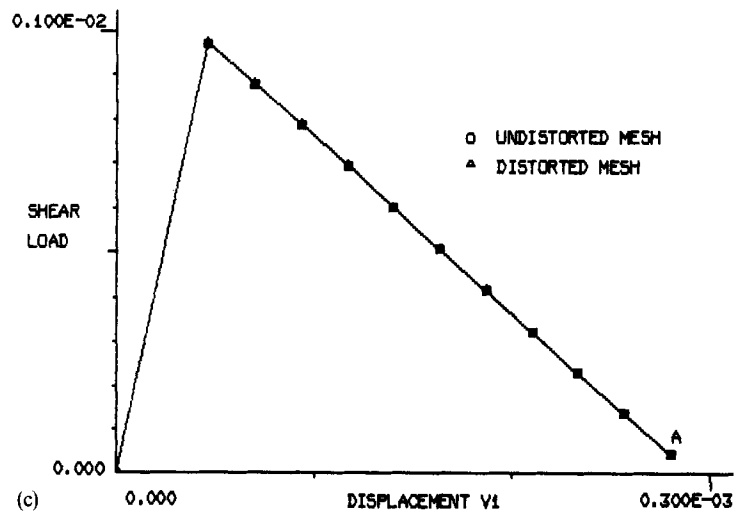

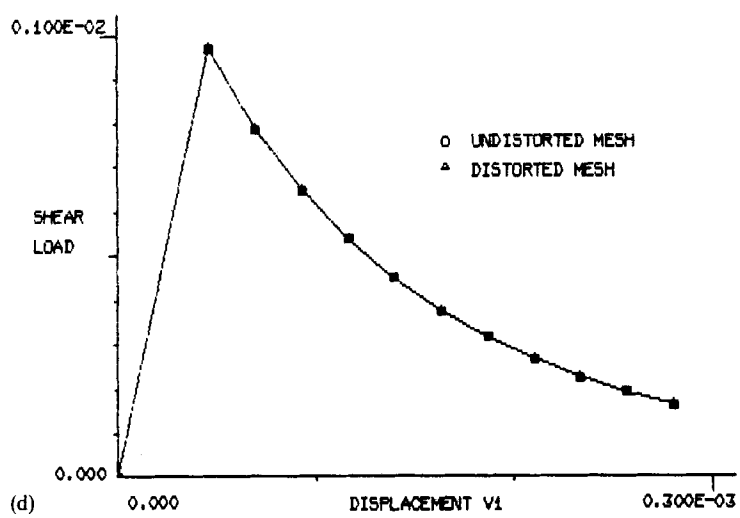

Figure 6(a, b, c, d)

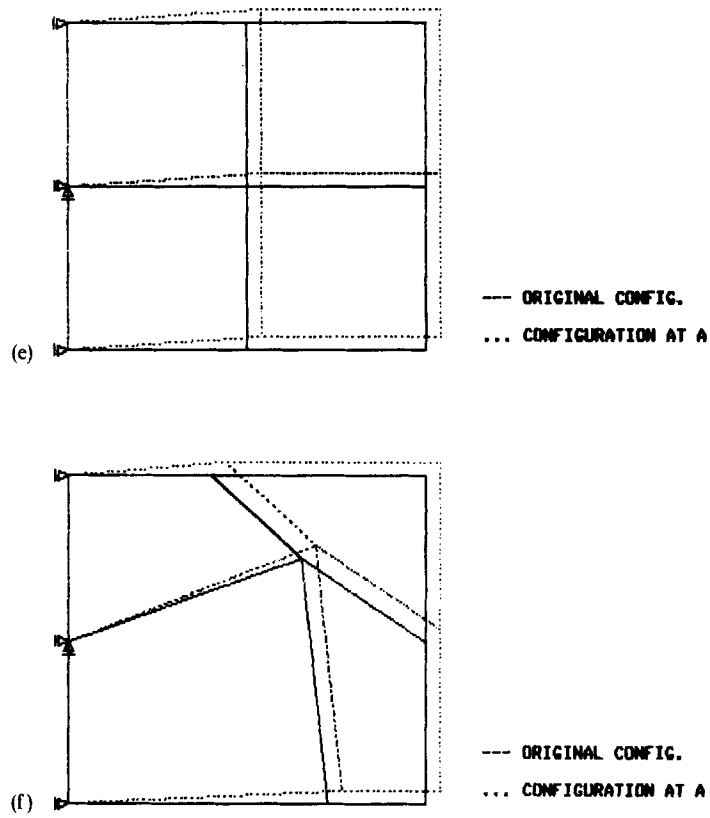

Figure 6. Pure shear in four element meshes (plane stress): (a) undistorted mesh; (b) distorted mesh; (c) results corresponding to a linear $\hat{r}$–$\hat{v}$ relation; (d) results corresponding to a non-linear $\hat{r}$–$\hat{v}$ relation; (e) final equilibrium configuration of undistorted mesh; (f) final equilibrium configuration of distorted mesh

Iterating using only the symmetric component of the stiffness matrix

In order to compare the efficiencies of the solution procedure when the consistent stiffness matrix is used and when only its symmetric component is used, we consider the following cases:

(i) biaxial stress state (Figure 5) with linear $\hat{r}$–$\hat{v}$ relation;
(ii) biaxial stress state (Figure 5) with exponential $\hat{r}$–$\hat{v}$ relation;
(iii) pure shear (Figure 6) with linear $\hat{r}$–$\hat{v}$ relation;
(iv) pure shear (Figure 6) with exponential $\hat{r}$–$\hat{v}$ relation.

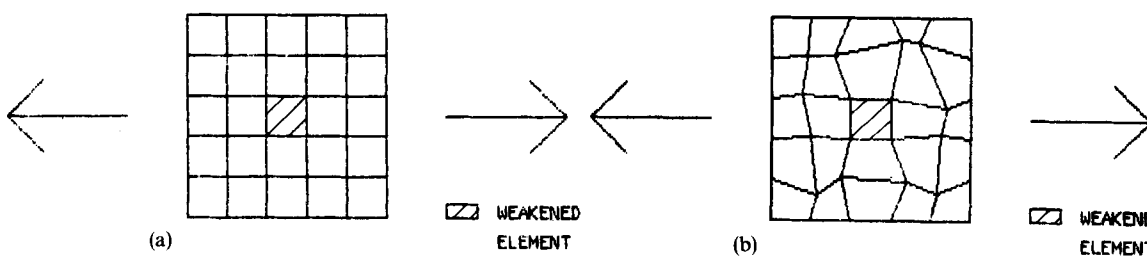

Figure 7(a, b)

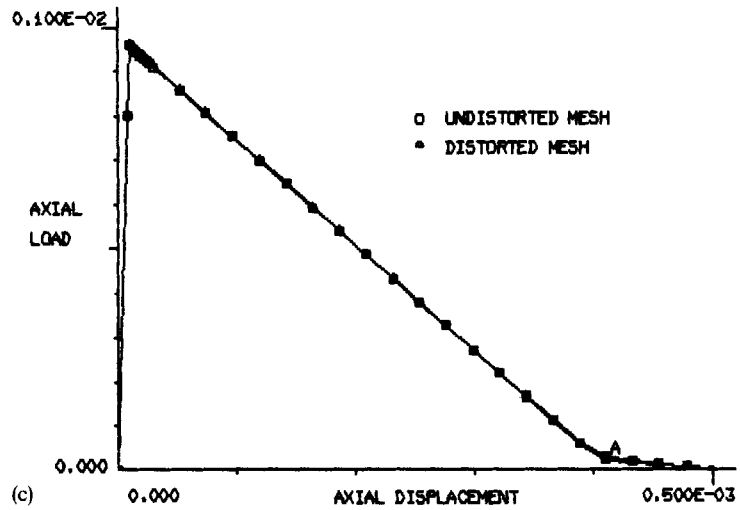

(c)

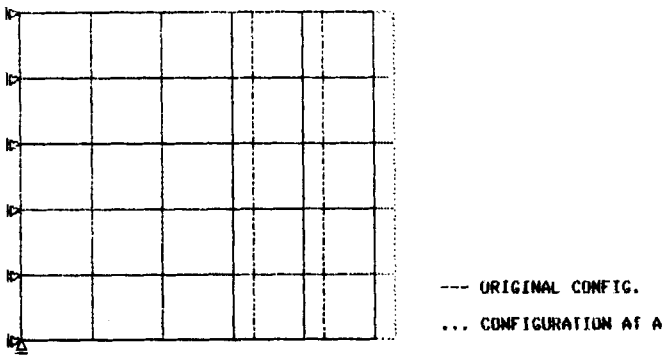

(d)

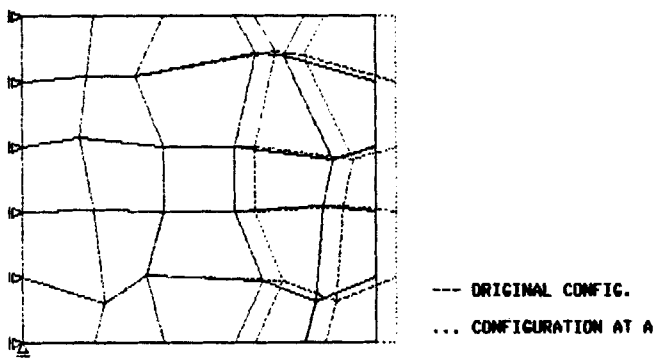

(e)

Figure 7. Tensile load in large meshes (plane stress): (a) undistorted mesh; (b) distorted mesh; (c) results corresponding to a linear $\hat{r}$–$\hat{v}$ relation; (d) final equilibrium configuration of undistorted mesh; (e) final equilibrium configuration of distorted mesh

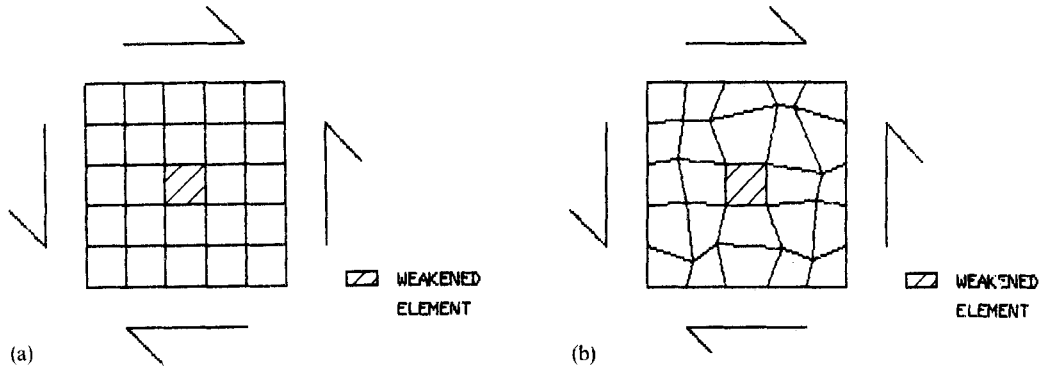

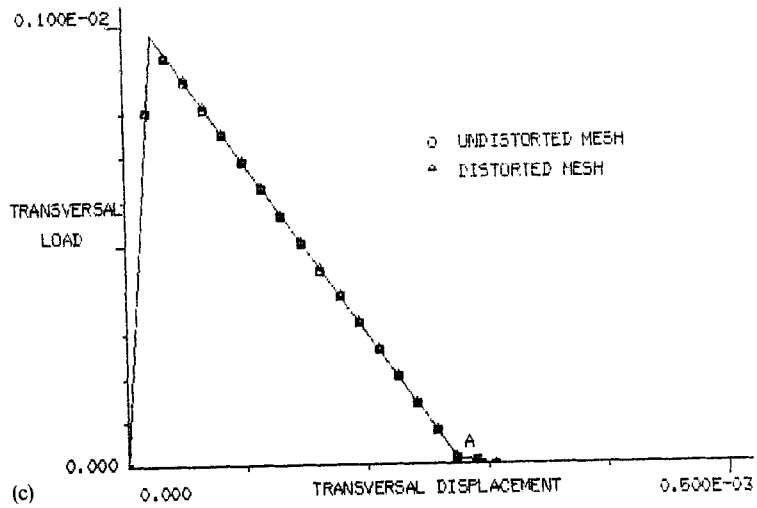

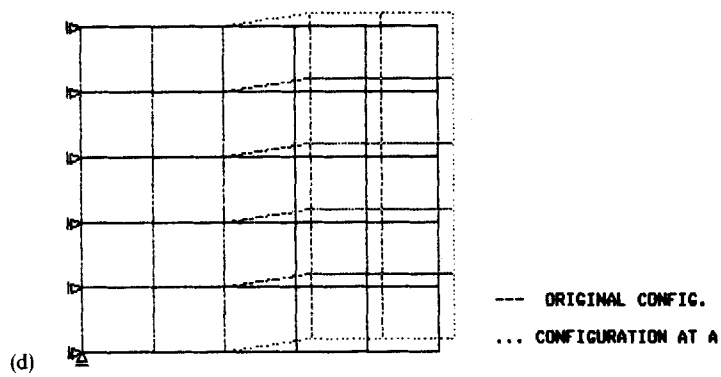

Figure 8(a, b, c, d)

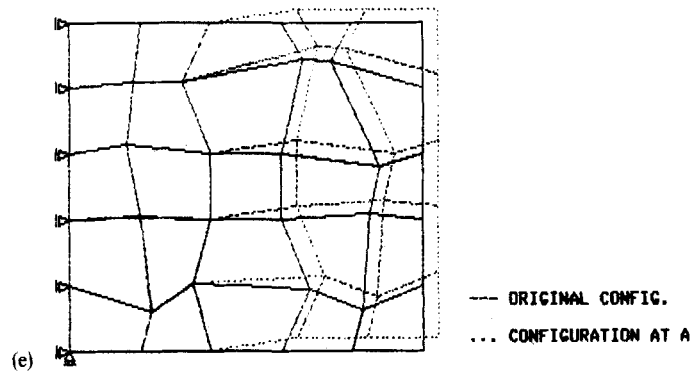

Figure 8. Pure shear in large meshes (plane stress): (a) undistorted mesh; (b) distorted mesh; (c) results corresponding to a linear $\hat{r}$–$\hat{v}$ relation; (d) final equilibrium configuration of undistorted mesh; (e) final equilibrium configuration of distorted mesh

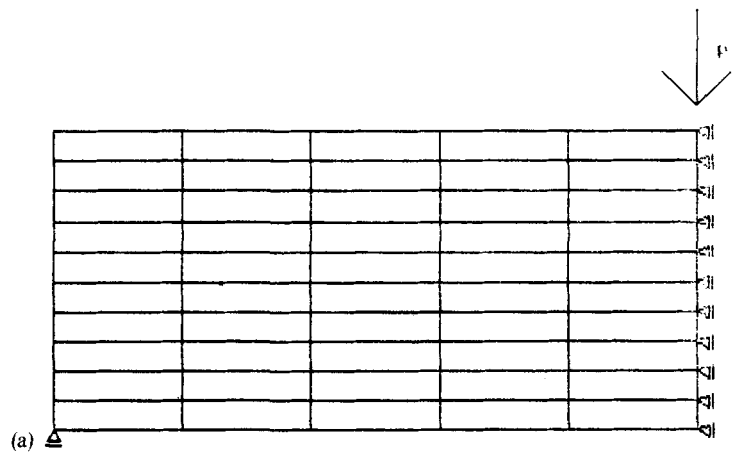

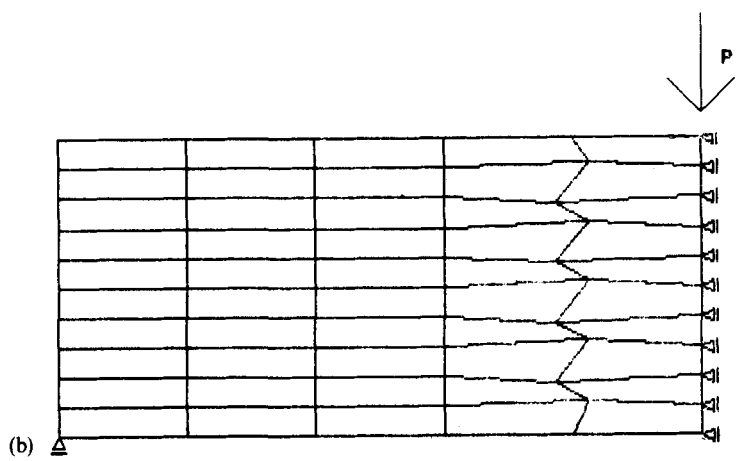

Figure 9(a, b)

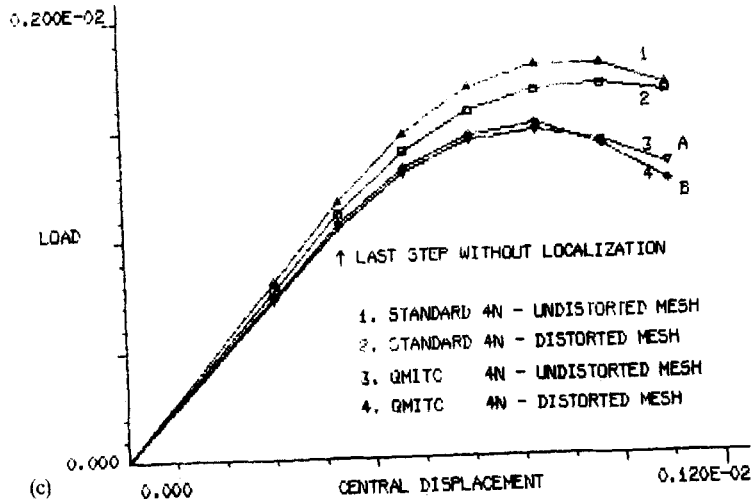

(c)

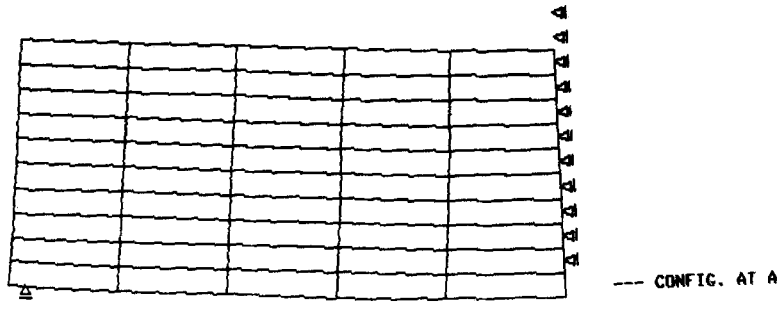

(d)

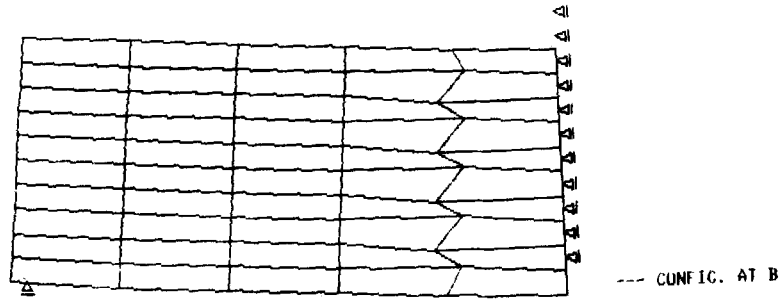

(e)

Figure 9. Bending of simply supported beam (plane stress): (a) undistorted mesh; (b) distorted mesh; (c) results corresponding to standard 4N and QMITC elements; (d) final equilibrium configuration of undistorted QMITC mesh; (e) final equilibrium configuration of distorted QMITC mesh

For each of the above cases we run the complete problem (from the unstressed initial configuration up to the final fractured configuration), iterating in the load displacement space[35] with different iterative schemes and an energy tolerance ETOL = 1·e − 10. In all cases we use 11 steps, a first step close to the localization point and 10 more equal steps. In Tables I to IV, for each

Table I

Iteration method	$\mathbf{K}_C$	$\mathbf{K}_S$	$\mathbf{K}_E$
Newton–Raphson	8/1	10/8	—
B.F.G.S.[29]	—	—	10/12
Modified N–R	28/1	28/8	28/29

Table II

Iteration method	$\mathbf{K}_C$	$\mathbf{K}_S$	$\mathbf{K}_E$
Newton–Raphson	7/2	10/8	—
B.F.G.S.	—	—	10/11
Modified N–R	29/3	29/8	29/30

Table III

Iteration method	$\mathbf{K}_C$	$\mathbf{K}_S$	$\mathbf{K}_E$
Newton–Raphson	5/1	13/10	—
B.F.G.S.	—	—	15/13
Modified N–R	80/1	80/12	80/80

Table IV

Iteration method	$\mathbf{K}_C$	$\mathbf{K}_S$	$\mathbf{K}_E$
Newton–Raphson	4/2	11/10	—
B.F.G.S.	—	—	15/13
Modified N–R	88/3	88/10	88/69

of the above cases, we indicate for the different combinations of iterative procedures and stiffness matrices the pair of numbers 'a/b' where

a: number of iterations in the second step where the localization is triggered.
b: average number of iterations in each of the following 9 steps.

In these tables,

$\mathbf{K}_C$: consistent stiffness matrix;
$\mathbf{K}_S$: symmetric part of the consistent stiffness matrix;
$\mathbf{K}_E$: elastic stiffness matrix.

The conclusion is that, although the consistent stiffness matrix provides a more efficient solution scheme, the efficiency provided by its symmetric part only is still acceptable.

4. CONCLUSIONS

In previous publications we presented finite element formulations for certain solid mechanics problems that fulfil a number of requirements that render those formulations a reliable modelling tool in engineering applications.[25–28,37] Those requirements were stated as follows.

1. The theoretical formulation of the elements is clear, and does not incorporate numerically adjusted factors.
2. The elements do not contain any spurious zero energy mode.
3. The elements satisfy Irons' patch test.
4. The elements are relatively insensitive to distortions and changes in material properties (e.g. no locking in plane strain plasticity).

In this paper we develop a formulation for localization problems that also fulfils the above reliability criteria.

Following the basic ideas of the discrete crack approach (Hillerborg) and of the smeared crack approach (Bažant), we developed a new formulation for solving strain localization problems. This new formulation introduces displacement interpolated localization lines embedded in the element domains.

For the localization lines a local stress–displacement constitutive relation is used, assuring in the case of fracture problems a correct energy dissipation, and in this sense, the new formulation is equivalent to the preceding ones, keeping objectivity with regard to regular mesh refinements.

The advantage of the new formulation over the discrete crack approach is that it does not need mesh redefinitions to follow the progression of the localization zone; and the advantage over the smeared crack approach is that it can deal with distorted meshes without causing deterioration of the results.

Although the new formulation introduces a non-symmetric consistent stiffness matrix, our numerical experimentation shows that, with a limited efficiency decrease, only the symmetric part of the consistent stiffness matrix can be used. This makes the finite elements with embedded localization lines easy to implement in standard non-linear finite element codes, and therefore all the existing finite element libraries and constitutive models for the material outside the localization line can be readily used in combination with them.

Although in this paper we experimented only with fracture problems we are presently working on the extension of this finite element formulation to shear-band problems in which the localization is triggered by material instability.

ACKNOWLEDGEMENT

This research was carried out in the framework of a joint research agreement between the Instituto de Materiales y Estructuras and the Instituto Nacional de Tecnología Industrial, Buenos Aires, Argentina.

REFERENCES

1. W. F. Chen, *Plasticity in Reinforced Concrete*, McGraw-Hill, New York, 1982.
2. J. G. Van Mier, 'Strain softening of concrete under multiaxial loading conditions', *Doctoral Thesis*, Eindhoven University of Technology, The Netherlands, 1984.
3. Z. P. Bažant, 'Size effect in blunt fracture: Concrete, rock and metal', *J. Eng. Mech. ASCE*, **110**, 518–534 (1984).
4. St. Pietruszczak and Z. Mroz, 'Finite element analysis of deformation of strain-softening materials', *Int. j. numer. methods eng.*, **17**, 327–334 (1981).
5. M. Ortiz, Y. Leroy and A. Needleman, 'A finite element method for localized failure analysis', *J. Comp. Methods Appl. Mech. Eng.*, **61**, 189–214 (1987).
6. A. Needleman, 'Dynamic shear band development in plane strain', *J. Appl. Mech. ASME*, **56**, 1–9 (1989).
7. T. Belytschko, J. Fish and B. E. Engelman, 'A finite element with embedded localization zones', *J. Comp. Methods Appl. Mech. Eng.*, **70**, 59–89 (1988).
8. Z. P. Bažant, 'Stable states and paths of structures with plasticity or damage', *J. Eng. Mech. ASCE*, **114**, 2013–2034 (1988).
9. Z. P. Bažant, 'Instability, ductility and size effect in strain softening concrete', *J. Eng. Mech. Div. ASCE*, **102**, 331–344 (1976); discussions, **103**, 357–358, 775–777 (1976); **104**, 501–502 (1976).
10. N. S. Ottosen, 'Thermodynamic consequences of strain softening in tension', *J. Eng. Mech. ASCE*, **112**, 1152–1164 (1986).
11. Z. P. Bažant, 'Mechanics of distributed cracking', *ASME Appl. Mech. Rev.*, **39**, 675–705 (1986).
12. Z. P. Bažant and P. A. Pfeiffer, 'Determination of fracture energy from size effect and brittleness number', *ACI Mater. J.*, **84**, 463–480 (1987).
13. G. Pijaudier-Cabot, Z. P. Bažant and M. Tabbara, 'Comparison of various models for strain softening', *Eng. Comp.*, **5**, 141–150 (1988).
14. Y. R. Rashid, 'Analysis of prestressed concrete pressure vessels', *Nucl. Eng. Des.*, **7**, 334–355 (1968).
15. Z. P. Bažant and B. H. Oh, 'Crack band theory for fracture of concrete', *RILEM Mater. Struct.*, **16**, 155–177 (1983).
16. Z. P. Bažant and B. H. Oh, 'Rock fracture via strain-softening finite elements', *J. Eng. Mech. ASCE*, **110**, 1015–1035 (1984).
17. J. Oliver, 'A consistent characteristic length for smeared cracking models', *Int. j. numer. methods eng.*, **28**, 461–474 (1989).
18. A. Hillerborg, M. Modéer and P. E. Petersson, 'Analysis of crack formation and crack growth in concrete by means of fracture mechanics and finite elements', *Cement Concr. Res.*, **6**, 773–782 (1976).
19. A. R. Ingraffea and V. Saouma, 'Numerical modeling of discrete crack propagation in reinforced and plain concrete', in G. C. Sih and A. Tommaso (eds.), *Fracture Mechanics of Concrete: Structural Application and Numerical Calculation*, Martinus Nijhoff, Dordrech, The Netherlands, 1985.
20. K. J. William, N. Bicanic and S. Sture, 'Constitutive and computational aspects of strain softening and localization in solids', in K. J. William (ed.), *Constitutive Equations: Macro and Computational Aspects*, ASME, New York, 1984.
21. J. W. Hutchinson, *A Course on Nonlinear Fracture Mechanics*, The Technological University of Denmark, 1979.
22. E. N. Dvorkin, R. J. Torrent and A. M. Alvaredo, 'A constitutive relation for concrete', in D. R. J. Owen *et al.* (eds.), *Proc. 1st Int. Conf. on Computational Plasticity*, Pineridge Press, Swansea, U.K., 1987.
23. R. J. Torrent, E. N. Dvorkin and A. M. Alvaredo, 'A model for work hardening plasticity and fracture of concrete under multiaxial stresses', *Cement Concr. Res.*, **17**, 939–950 (1987).
24. E. N. Dvorkin, A. M. Cuitiño and G. Gioia, 'A concrete material model based on non-associated plasticity and fracture', *Eng. Comp.*, **6**, 281–294 (1989).
25. E. N. Dvorkin and K. J. Bathe, 'A continuum mechanics based four-node shell element for general nonlinear analysis', *Eng. Comp.*, **1**, 77–88 (1984).
26. K. J. Bathe and E. N. Dvorkin, 'A four-node plate bending element based on Mindlin–Reissner plate theory and a mixed interpolation', *Int. j. numer. methods eng.*, **21**, 367–383 (1985).
27. K. J. Bathe and E. N. Dvorkin, 'A formulation of general shell elements—The use of mixed interpolation of tensorial components', *Int. j. numer. methods eng.*, **22**, 697–722 (1986).
28. E. N. Dvorkin and S. I. Vassolo, 'A quadrilateral 2D finite element based on mixed interpolation of tensorial components', *Eng. Comp.*, **6**, 217–224 (1989).
29. K. J. Bathe, *Finite Element Procedures in Engineering Analysis*, Prentice-Hall, Englewood Cliffs, N.J., 1982.
30. R. L. Taylor, J. C. Simo, O. C. Zienkiewicz and A. C. Chan, 'The patch test. A condition for assessing FEM convergence', *Int. j. numer. methods eng.*, **22**, 39–62 (1986).

31. B. M. Irons and A. Razzaque, 'Experience with the patch test for convergence of finite elements', in A. K. Aziz (ed.), *The Mathematical Foundation of Finite Element Methods with Application to Partial Differential Equations*, Academic Press, New York, 1972.
32. Z. P. Bažant and F. B. Lin, 'Nonlocal smeared cracking model for concrete fracture', *J. Struct. Eng. ASCE*, **114**, 2493–2510 (1988).
33. G. Pijaudier-Cabot, and Z. P. Bažant, 'Nonlocal damage theory', *J. Eng. Mech. ASCE*, **113**, 1512–1533 (1987).
34. K. Washizu, *Variational Methods in Elasticity and Plasticity*, 3rd edn, Pergamon Press, New York, 1982.
35. K. J. Bathe and E. N. Dvorkin, 'On the automatic solution of nonlinear finite element equations', *Comp. Struct.*, **17**, 871–879 (1983).
36. G. N. Pande and St. Pietruszczak, 'Symmetric tangential stiffness formulation for non-associated plasticity', *Comp. Geotechnics*, **2**, 89–99 (1986).
37. E. N. Dvorkin and A. P. Assanelli, 'Elasto-plastic analysis using a quadrilateral 2D element based on mixed interpolation of tensorial components', in D. R. J. Owen *et al.* (eds.), *Proc. 2nd Int. Conf. on Computational Plasticity* Pineridge Press, Swanasea, U.K., 1989.